1

Harmonic lasing in X-ray FELs: theory and experiment

E. A. Schneidmiller* and M .V. Yurkov

*Deutsches Elektronen-Synchrotron (DESY),
Notkestrasse 85, D-22607 Hamburg, Germany*
*E-mail: evgeny.schneidmiller@desy.de

Harmonic lasing is a perspective mode of operation of X-ray FEL user facilities that allows to provide brilliant beams of higher energy photons for user experiments. Another useful application of harmonic lasing is so called Harmonic Lasing Self-Seeded Free Electron Laser (HLSS FEL) that allows to improve spectral brightness of these facilities. In the past, harmonic lasing has been demonstrated in the FEL oscillators in infrared and visible wavelength ranges, but not in high-gain FELs and not at short wavelengths. In this paper we report on the first evidence of the harmonic lasing and the first operation of the HLSS FEL at the soft X-ray FEL user facility FLASH in the wavelength range between 4.5 nm and 15 nm. Spectral brightness was improved in comparison with Self-Amplified Spontaneous emission (SASE) FEL by a factor of six in the exponential gain regime. A better performance of HLSS FEL with respect to SASE FEL in the post-saturation regime with a tapered undulator was observed as well. The first demonstration of harmonic lasing in a high-gain FEL and at short wavelengths paves the way for a variety of applications of this new operation mode in X-ray FELs.

1. Introduction

Successful operation of X-ray free electron lasers (FELs)[1–3], based on self-amplified spontaneous emission (SASE) principle[4], down to an Ångström regime opens up new horizons for photon science. Even shorter wavelengths are requested by the scientific community.

One of the most promising ways to extend the photon energy range of high-gain X-ray FELs is to use harmonic lasing which is the FEL instability at an odd harmonic of the planar undulator[5–9] developing independently from the lasing at the fundamental. Contrary to the nonlinear harmonic generation[1,6,7,10–13] (which is driven by the fundamental in the vicinity of saturation), harmonic lasing can provide much more intense, stable, and narrow-band radiation if the fundamental is suppressed. The most attractive feature of saturated harmonic lasing is that the spectral brightness of a harmonic is comparable to that of the fundamental[9].

Another interesting option, proposed in[9], is the possibility to improve spectral brightness of an X-ray FEL by the combined lasing on a harmonic in the first part of the undulator (with an increased undulator parameter K) and on the fundamental in the second part of the undulator. Later this concept was named Harmonic Lasing Self-Seeded FEL (HLSS FEL)[14]. Even though this scheme is not expected to provide an ultimate monochromatization of the FEL radiation as do self-seeding schemes using optical elements[15–17], it has other advantages that we briefly discuss below in the paper.

2

Harmonic lasing was initially proposed for FEL oscillators[18] and was tested experimentally in infrared and visible wavelength ranges[19–22]. It was, however, never demonstrated in high-gain FELs and at a short wavelength. In this paper we present the first successful demonstration of this effect at the second branch of the soft X-ray FEL user facility FLASH[23] where we managed to run HLSS FEL in the wavelength range between 4.5 nm and 15 nm.

2. Harmonic lasing

Harmonic lasing in single-pass high-gain FELs[5–9] is the amplification process of higher odd harmonics developing independently of each other (and of the fundamental harmonic) in the exponential gain regime. In the case of a SASE FEL the fluctuations of the beam current with frequency components in the vicinity of a wavelength

$$\lambda_h = \frac{\lambda_{\mathrm{w}}(1 + K^2)}{2h\gamma^2} \qquad h = 1, 3, 5...$$ (1)

serve as an input signal for amplification process. Here λ_{w} is the undulator period, γ is relativistic factor, h is harmonic number, and K is the rms undulator parameter:

$$K = 0.934 \ \lambda_{\mathrm{w}}[\mathrm{cm}] \ B_{\mathrm{rms}}[\mathrm{T}] \ ,$$

B_{rms} being the rms undulator field (peak field divided by $\sqrt{2}$ for a planar undulator with the sinusoidal field).

An advantage of harmonic lasing over lasing on the fundamental at the same wavelength can be demonstrated for the case of a gap-tunable undulator. In this case one uses a higher K-value for harmonic lasing, i.e. for the lasing on the fundamental one has to reduce K to the value K_{re}:

$$K_{re}^2 = \frac{1 + K^2}{h} - 1 \ .$$ (2)

Obviously, K must be larger than $\sqrt{h-1}$.

Then one can derive a ratio of the gain length of the fundamental, $L_g^{(1)}$, to the gain length of a harmonic $L_g^{(h)}$[9]:

$$\frac{L_g^{(1)}}{L_g^{(h)}} = \frac{h^{1/2}K A_{JJh}(K)}{K_{re} A_{JJ1}(K_{re})} \ .$$ (3)

Here $A_{JJh}(K) = J_{(h-1)/2}\left(\frac{hK^2}{2(1+K^2)}\right) - J_{(h+1)/2}\left(\frac{hK^2}{2(1+K^2)}\right)$ is the coupling factor for harmonics with J_n being Bessel functions. The coupling factors for the 1st, 3rd, and 5th harmonics are shown in Fig. 1.
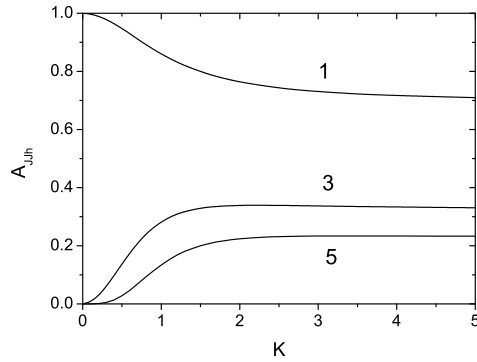
Fig. 1.   Coupling factors for the 1st, 3rd, and 5th harmonics (denoted with 1, 3, and 5, correspondingly) versus rms undulator parameter.
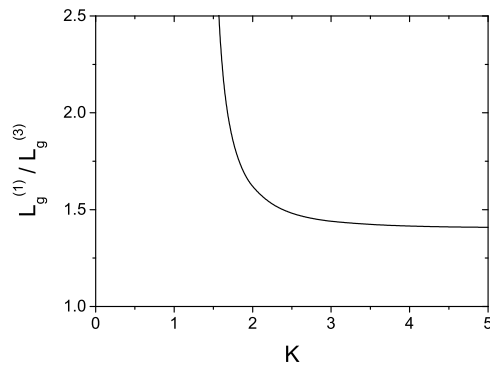

Fig. 2.   Ratio of the gain length of the retuned fundamental to the gain length of the third harmonic (3) for lasing at the same wavelength versus rms undulator parameter K. The ratio is derived in the frame of the three-dimensional theory for an optimized beta-function and negligible energy spread[9].

The formula (3) is obtained in the frame of the three-dimensional theory including diffraction of the radiation, emittance, betatron motion (and for an optimized beta-function) but assuming a negligible energy spread. The plot of the ratio of gain lengths (3) is presented in Fig. 2. It is clearly seen that harmonic lasing has always a shorter gain length under above mentioned conditions (and the ratio is larger than that obtained in one-dimensional model[8]). The ratio shown in Fig. 2 starts to diverge rapidly for the values of K approaching $\sqrt{2}$, and lasing at the fundamental becomes impossible below this point. However, there still remains a reserve in the value of parameter K allowing effective lasing at the third harmonic.

Amplification process of harmonics degrades with the increase of the energy
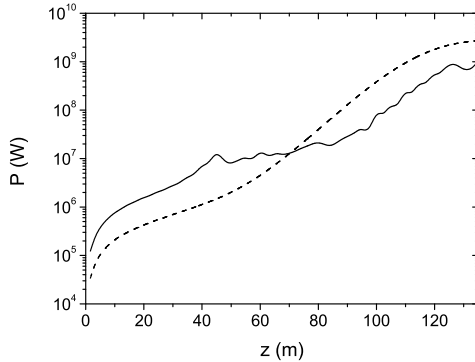
4

Fig. 3.   An example for the European XFEL. Averaged peak power for the fundamental harmonic (solid) and the third harmonic (dash) versus magnetic length of SASE1 undulator. The wavelength of the third harmonic is 0.2 Å (photon energy 62 keV). The fundamental is disrupted with the help of phase shifters installed after 5 m long undulator segments. The phase shifts are $4\pi/3$ after segments 1-8 and 21-26, and $2\pi/3$ after segments 9-16. Simulations were performed with the code FAST.

spread in the electron beam more rapidly than that of the fundamental. However, in practical situations there is always the range of parameters for which the harmonic lasing still has an advantage[9].

The most attractive feature of the saturated harmonic lasing is that the spectral brightness (or brilliance) of harmonics is comparable to that of the fundamental[9]. Indeed, a good estimate for the saturation efficiency is $\lambda_{\mathrm{w}}/(hL_{\mathrm{sat},h})$, where $L_{\mathrm{sat},h}$ is the saturation length of a harmonic ($h = 1$ for the fundamental). At the same time, the relative rms bandwidth has the same scaling. In other words, reduction of power is compensated by the bandwidth reduction, and the spectral power remains the same. If we consider the lasing at the same wavelength on the fundamental and on a harmonic (with the retuned undulator parameter K), transverse coherence properties are about the same since they are mainly defined by the emittance-to-wavelength ratio[55,56]. Thus, also the spectral brightness is about the same in both cases.

For a successful harmonic lasing to saturation, the fundamental must be suppressed. There have been different approaches proposed:

- phase shifters disrupting the fundamental but transparent for a harmonic[8,11];
- spectral filtering when a filter is put into a chicane[11];
- switching between the 3rd and the 5th harmonics[24,25].

Although known theoretically for a long time[5–8], harmonic lasing in high-gain FELs was never demonstrated experimentally. Moreover, it was never considered for practical applications in X-ray FELs. The situation was changed after publication of ref.[9] where it was concluded that the harmonic lasing in X-ray FELs is much more robust than usually thought, and can be effectively used in the existing and

future X-ray FELs. In particular, the European XFEL[26] can greatly outperform the specifications in terms of the highest possible photon energy: it can reach 60-100 keV range for the third harmonic lasing, see Fig. 3. It was also shown[24] that one can keep sub-Ångström range of operation of the European XFEL after CW upgrade of the accelerator with a reduction of electron energy from 17.5 GeV to 7 GeV. Another application of harmonic lasing is a possible upgrade of FLASH[27] with the aim to increase the photon energy up to 1 keV with the present energy 1.25 GeV of the accelerator. To achieve this goal, one should install a specially designed undulator optimized for the third harmonic lasing as suggested in Ref.[28].

3. Gain length of harmonic lasing

3.1. *Explicit formulas*

The results of this Section are generalizations of the results of Ref.[29] for the fundamental to the case of harmonic lasing. The eigenvalue equation[7] and the approach to its parametrization are discussed in Ref.[9]. In what follows we assume that the harmonic with a number h lases to saturation, while lasing at harmonics with lower numbers and at the fundamental is suppressed with the help of phase shifters or by other means (see Ref.[9]). We also assume that the beta-function is optimized so that the FEL gain length at a considered harmonic achieves the minimum for given wavelength, beam and undulator parameters. Under this condition the solution of the eigenvalue equation for the **field** gain length* of the TEM_{00} mode can be approximated as follows:

$$L_g \simeq L_{g0} \left(1 + \delta\right) , \qquad (4)$$

where

$$L_{g0} = 1.67 \left(\frac{I_A}{I}\right)^{1/2} \frac{(\epsilon_n \lambda_{\mathrm{w}})^{5/6}}{\lambda_h^{2/3}} \frac{(1 + K^2)^{1/3}}{h^{5/6} K A_{JJh}} , \qquad (5)$$

and

$$\delta = 131 \frac{I_A}{I} \frac{\epsilon_n^{5/4}}{\lambda_h^{1/8} \lambda_{\mathrm{w}}^{9/8}} \frac{h^{9/8} \sigma_\gamma^2}{(K A_{JJh})^2 (1 + K^2)^{1/8}} . \qquad (6)$$

The following notations are introduced here: $I_A = 17$ kA is the Alfven current, $\epsilon_n = \gamma \epsilon$ is the rms normalized emittance, $\sigma_\gamma = \sigma_\varepsilon / mc^2$ is the rms energy spread (in units of the rest energy), and

---

*e-folding length for the field amplitude. There is also a notion of the power gain length which is twice shorter.

6

$$A_{JJh}(K) = J_{(h-1)/2}\left(\frac{hK^2}{2(1+K^2)}\right) - J_{(h+1)/2}\left(\frac{hK^2}{2(1+K^2)}\right)$$

is the usual coupling factor for harmonics with J_n being Bessel functions. The coupling factors for the 1st, 3rd, and 5th harmonics are shown in Fig. 1. When the rms undulator parameter K is large, the coupling factors are $A_{JJ1} \simeq 0.696$, $A_{JJ3} \simeq 0.326$, $A_{JJ5} \simeq 0.230$. Asymptotically for large h we have $A_{JJh} \simeq 0.652\, h^{-2/3}$. Also note that all the formulas of this Section are valid in the case of helical undulator and the fundamental ($h = 1$), in this case the coupling factor is equal to 1.

The formulas (4)-(6) provide an accuracy better than 5 % in the range of parameters

$$1 < \frac{2\pi\epsilon}{\lambda_h} < 5 \ , \tag{7}$$

$$\delta < 2.5 \left\{1 - \exp\left[-\frac{1}{2}\left(\frac{2\pi\epsilon}{\lambda_h}\right)^2\right]\right\} \tag{8}$$

In fact, the formulas (4)-(6) can also be used well beyond this range, but the above mentioned accuracy is not guaranteed.

We also present here an approximate expression for the optimal beta-function (an accuracy is about 10 % in the above mentioned parameter range):

$$\beta_{\mathrm{opt}} \simeq 11.2\left(\frac{I_A}{I}\right)^{1/2} \frac{\epsilon_n^{3/2}\lambda_{\mathrm{w}}^{1/2}}{\lambda_h h^{1/2} K A_{JJh}}\,(1+8\delta)^{-1/3} \tag{9}$$

To estimate the saturation length, one can use the result from Ref. [30], generalized to the case of harmonic lasing:

$$L_{\mathrm{sat}} \simeq 0.6\, L_g \ln\left(hN_{\lambda_h}\frac{L_g}{\lambda_{\mathrm{w}}}\right)\ . \tag{10}$$

Here N_{λ_h} is a number of electrons per wavelength of the considered harmonic. For operating VUV and X-ray SASE FELs one typically has $L_{\mathrm{sat}} \simeq (10 \pm 1) \times\ L_g$.

Let us note that all the above presented results are reduced to those of Ref. [29] for the case of the first harmonic ($h = 1$). All these results were obtained under the assumption that beta-function is optimal (i.e. it is given by Eq. (9)). However, for technical reasons this is not always the case in real machines, and it could often be that $\beta > \beta_{\mathrm{opt}}$. In such a case the gain length can be approximated as follows:

$$L_g(\beta) \simeq L_g(\beta_{\mathrm{opt}})\left[1 + \frac{(\beta - \beta_{\mathrm{opt}})^2(1+8\delta)}{4\beta_{\mathrm{opt}}^2}\right]^{1/6} \qquad \text{for}\ \ \beta > \beta_{\mathrm{opt}} \tag{11}$$

3.2. *Generalization of Ming Xie formulas*

In Refs.[31,32] the fitting formulas were presented that approximate FEL **power** gain length, L_g. Note that in our parametrization in Section 3.1 we use the same notation for the **field** gain length which is twice longer. The power gain length of the fundamental harmonic was expressed in[31,32] as follows:

$$\frac{L_{1d}}{L_g} = \frac{1}{1 + \Lambda(\eta_d, \eta_\epsilon, \eta_\gamma)} \ , \tag{12}$$

where L_{1d} is the 1D gain length for the cold beam, and Λ depends on the three dimensionless parameters: η_d, η_ϵ, and η_γ. This dependence can be found in[31,32], it was obtained by fitting the solution of the eigenvalue equation with the help of 19 fitting coefficients.

We can generalize these results for calculation of power gain length $L_g^{(h)}$ of harmonic lasing in a simple way. Eq. (12) can be generalized as

$$\frac{L_{1d}^{(h)}}{L_g^{(h)}} = \frac{1}{1 + \Lambda(\eta_d^{(h)}, \eta_\epsilon^{(h)}, \eta_\gamma^{(h)})} \ . \tag{13}$$

The 1D gain length of harmonics can be calculated as

$$L_{1d}^{(h)} = \left(\frac{A_{JJ1}^2}{h A_{JJh}^2} \right)^{1/3} L_{1d} \ ,$$

and the function Λ now depends on the three generalized parameters:

$$\eta_d^{(h)} = \left(\frac{A_{JJ1}^2}{h A_{JJh}^2} \right)^{1/3} \frac{\eta_d}{h} \qquad \eta_\epsilon^{(h)} = \left(\frac{A_{JJ1}^2}{h A_{JJh}^2} \right)^{1/3} h\eta_\epsilon \qquad \eta_\gamma^{(h)} = \left(\frac{A_{JJ1}^2}{h A_{JJh}^2} \right)^{1/3} h\eta_\gamma$$

Comparing two approaches to parametrization of FEL gain length, we have found that they agree reasonably well, also for non-optimal beta-functions and well beyond the range given by Eq. (7). As an example, we present a comparison for the case of LCLS. The main parameters are as follows[2]: undulator period is 3 cm, rms undulator parameter is 2.475, peak current of the electron bunch is 3 kA, normalized emittance is 0.4 mm mrad, slice energy spread is 1.4 MeV. Beta function scales with electron energy as $\beta[m] = 30\frac{E[GeV]}{13.6}$. In Fig. 4 we present the power gain length versus wavelength for lasing at the fundamental and at the third harmonic, calculated with our formulas and with generalized Ming Xie formulas. One can notice a good agreement of two different parametrizations of the FEL gain length. It is also worth noticing that in the range of wavelengths 1.5 - 5 A the third harmonic gain length is slightly smaller than that of the fundamental (achieved at a larger electron energy).
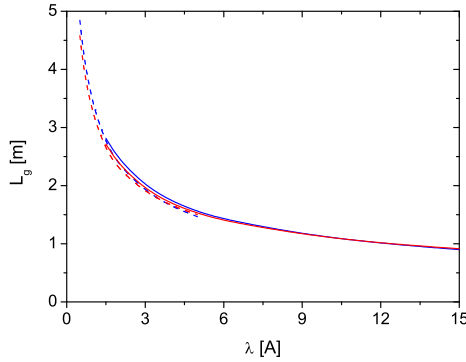
8

Fig. 4.   Power gain length of the fundamental (solid) and of the 3rd harmonic (dash) versus wavelength for LCLS. Shown in blue are results of calculation with our formulas, in red - with generalized Ming Xie formulas.

3.3. *Harmonic lasing of a thin electron beam*

For a typical operating range of hard X-ray FELs the condition $2\pi\epsilon/\lambda \simeq 1$ is usually a design goal for the shortest wavelength. In the case of the simultaneous lasing, the fundamental has shorter gain length than harmonics. However, if the same electron beam is supposed to drive an FEL in a soft X-ray beamline, the regime with $2\pi\epsilon/\lambda \ll 1$ is automatically achieved. Here we present a detailed study of this regime. In this Section we assume that beta-function is sufficiently large, $\beta \gg L_g^{(h)}$. In this case we can use the model of parallel beam (no betatron oscillations), and can also neglect an influence of longitudinal velocity spread due to emittance on FEL process. If in addition the energy spread is negligibly small, then the normalized FEL growth rate at the fundamental is described by the only dimensionless parameter, namely the diffraction parameter B [35]. The generalized diffraction parameter $\tilde{B}$, that can be used for harmonics, can be written as follows:

$$\tilde{B} = 2\epsilon\beta\tilde{\Gamma}\omega_h/c \ , \tag{14}$$

where $\omega_h = 2\pi c/\lambda_h$ and $\tilde{\Gamma}$ is the gain factor that also depends on harmonic number:

$$\tilde{\Gamma} = \left(\frac{A_{\mathrm{JJh}}^2 I \omega_h^2 K^2 (1 + K^2)}{I_{\mathrm{A}} c^2 \gamma^5} \right)^{1/2} \tag{15}$$

The gain length of a harmonic is defined by the universal function of $\tilde{B}$:

$$L_g^{(h)} = [\tilde{\Gamma} f_1(\tilde{B})]^{-1} \tag{16}$$

The function $f_1(\tilde{B})$ can be calculated from the eigenvalue equation presented in Ref. [35] for the Gaussian transverse distribution of current density (see Fig. 4.52 of

Ref.[35]). In the parameter range, that is the most interesting for our purpose, we can approximate the function $f_1(\tilde{B})$ as follows:

$$f_1(\tilde{B}) \simeq 0.66 - 0.37 \log_{10}(\tilde{B}) \qquad for \;\; \tilde{B} < 3 \; . \qquad (17)$$

Using the superscript (h) to indicate the harmonic number for the diffraction parameter and the gain factor, we can see that

$$\frac{\tilde{B}^{(h)}}{\tilde{B}^{(1)}} = \frac{h\tilde{\Gamma}^{(h)}}{\tilde{\Gamma}^{(1)}} = \frac{h^2 A_{JJh}}{A_{JJ1}} \; . \qquad (18)$$

According to (16) and (15), the ratio of gain lengths can be presented as follows:

$$\frac{L_g^{(1)}}{L_g^{(h)}} = \frac{h A_{JJh}}{A_{JJ1}} \frac{f_1(\tilde{B}^{(h)})}{f_1(\tilde{B}^{(1)})} \qquad (19)$$

One can easily observe from (18) and (19) that for a given value of diffraction parameter for the fundamental, $B = \tilde{B}^{(1)}$, this ratio depends only on the parameter K for a considered harmonic. If K is sufficiently large (see Fig. 1), one can obtain a universal dependence which is presented in Fig. 5 for the case of the third harmonic. For large values of the diffraction parameter (wide electron beam limit) one can use an asymptotic expression for the growth rate[35], so that the function f_1 is proportional to $(\tilde{B}^{(h)})^{-1/3}$. In this case one obtains the result of 1D theory[8]:

$$\frac{L_g^{(1)}}{L_g^{(h)}} \simeq \left(\frac{h A_{JJh}^2}{A_{JJ1}^2} \right)^{1/3} \; .$$

In the case of the third harmonic and large K this ratio is equal to 0.87. One can see that the curve in Fig. 5 slowly approaches this value when B is large. So, in the limit of wide electron beam, corresponding to 1D model, the fundamental has shorter gain length than harmonics.

In the limit of small diffraction parameter (thin electron beam) we wave the opposite situation, as one can see from Fig. 5. When diffraction parameter is smaller than 0.4, the gain length of the fundamental is larger than that of the third harmonic for large values of K. A similar dependence can be calculated for the fifth harmonic, in this case the gain length of the fundamental is larger than that of the fifth harmonic (for a sufficiently large K) when $B < 0.28$. Moreover, the fifth harmonic grows faster than the third one when $B < 0.15$ and K is large. In fact, if the diffraction parameter for the fundamental is about 0.1 or less, there might a number of amplified harmonics with similar growth rates. We should note that this number can be reduced when the energy spread is included into consideration.

To find out how the value of B, at which the harmonics have the same gain length as the fundamental, depends on the undulator parameter K, one can use the
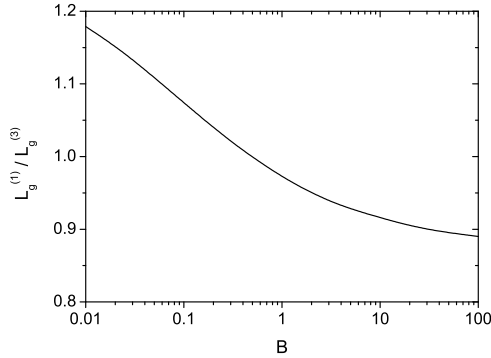
10

Fig. 5. Ratio of gain lengths for lasing at the fundamental and at the third harmonic versus diffraction parameter of the fundamental for large values of the undulator parameter K.
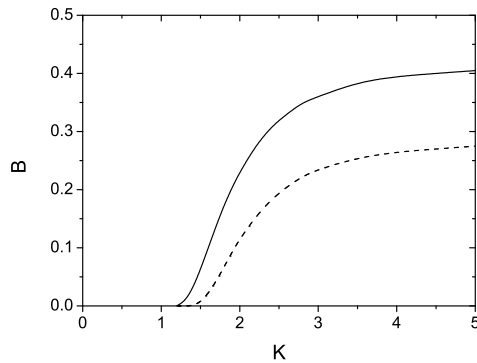

Fig. 6. Diffraction parameter of the fundamental, for which the third (solid) and the fifth (dash) harmonics have the same gain length as the fundamental, versus the rms undulator parameter K. Below these curves harmonics have shorter gain lengths than the fundamental.

Eqs. (17)-(19). We present the results for the third and the fifth harmonics in Fig. 6. The areas below the curves in Fig. 6 correspond to the case when corresponding harmonics grow faster than the fundamental. We should stress that the condition $2\pi\epsilon/\lambda \ll 1$ is necessary but not sufficient for reaching this regime.

In Fig. 7 we illustrate harmonic lasing at the small diffraction parameter, $B = 0.01$, and a large undulator parameter, $K \gg 1$.

Let us discuss why the effect, considered in this Section, can only take place in the frame of 3D theory and in the limit of a thin beam. In 1D theory the gain factor (inversely proportional to the gain length) scales as $(A_{JJh}^2 \omega_h)^{1/3}$, if we keep only parameters that depend on harmonic number. The frequency here comes from
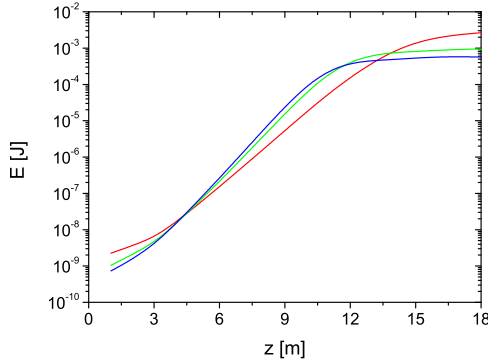
Fig. 7.   Illustration of harmonic lasing at the small diffraction parameter, $B = 0.01$, and a large undulator parameter, $K \gg 1$. FEL pulse energy versus undulator length is shown for the 1st (red), the 3rd (green), and the 5th (blue) harmonics.

the dynamical part of the problem, it reflects the fact that the beam gets bunched easier at higher frequencies. As for the electrodynamic part of the problem, the amplitude of the radiation field of charged planes does not depend on frequency. Since the product $A^2_{JJh}h$ decreases with harmonic number for any K, gain length of harmonics is always larger than that of the fundamental. Concerning the 3D theory, the solution of the paraxial wave equation shows that on-axis field amplitude is proportional to the frequency (what reflects the fact that the divergence is smaller for a higher frequency). So, both dynamical and electrodynamic parts contribute to the solution of the self-consistent problem with ω_h. That is why in the gain factor in Eq. (15) we have squared frequency $(A^2_{JJh}\omega^2_h)^{1/2}$, i.e. it depends on harmonic number via the product $A^2_{JJh}h^2$ which can increase with harmonic number if K is sufficiently large. Since in the case of a thin electron beam the function f_1 depends only weakly, in fact logarithmically, on the diffraction parameter (which is larger for harmonics), harmonics can grow faster than the fundamental in some range of parameters B and K, as it is illustrated in Fig. 6.

4. Harmonic lasing self-seeded FEL

A poor longitudinal coherence of SASE FELs [33–35] stimulated efforts for its improvement. Since an external seeding seems to be difficult to realize in X-ray regime, a so called self-seeding has been proposed [15–17]. There are alternative approaches for reducing bandwidth and increasing spectral brightness of X-ray FELs without using optical elements. One of them [37,38] suggests to use chicanes inside the undulator system to increase slippage of the radiation and to establish long-range correlations in the radiation pulse. Another method was proposed in [9] and is based on the combined lasing on a harmonic in the first part of the undulator (with increased undulator parameter K, see formula (2)) and on the fundamental in the second
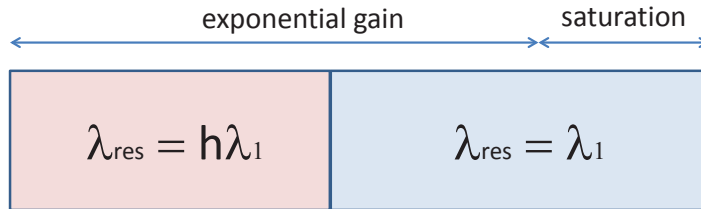
Fig. 8.   Conceptual scheme of a harmonic lasing self-seeded FEL

part. In this way the second part of the undulator is seeded by a narrow-band signal generated via a harmonic lasing in the first part. This concept was named HLSS FEL (Harmonic Lasing Self-Seeded FEL)[14]. Note that a very similar concept was proposed in[39] and was called a purified SASE FEL, or pSASE.

Typically, gap-tunable undulators are planned to be used in X-ray FEL facilities. If maximal undulator parameter K is sufficiently large, the concept of harmonic lasing self-seeded FEL can be applied in such undulators (see Fig. 8). An undulator is divided into two parts by setting two different undulator parameters such that the first part is tuned to a h-th sub-harmonic of the second part which is tuned to a wavelength of interest λ_1. Harmonic lasing occurs in the exponential gain regime in the first part of the undulator, also the fundamental in the first part stays well below saturation. In the second part of the undulator the fundamental is resonant to the wavelength, previously amplified as the harmonic. The amplification process proceeds in the fundamental up to saturation. In this case the bandwidth is defined by the harmonic lasing (i.e. it is reduced by a significant factor depending on harmonic number) but the saturation power is still as high as in the reference case of lasing at the fundamental in the whole undulator, i.e. the spectral brightness increases.

The enhancement factor of the coherence length (or, bandwidth reduction factor), that one obtains in HLSS FEL in comparison with a reference case of lasing in SASE FEL mode in the whole undulator, reads[14]:

$$R \simeq h \, \frac{\sqrt{L_{\mathrm{w}}^{(1)} L_{\mathrm{sat},h}}}{L_{\mathrm{sat},1}} \tag{20}$$

Here h is harmonic number, $L_{\mathrm{sat},1}$ is the saturation length in the reference case of the fundamental lasing with the lower K-value, $L_{\mathrm{w}}^{(1)}$ is the length of the first part of the undulator, and $L_{\mathrm{sat},h}$ is the saturation length of harmonic lasing. We notice that it is beneficial to increase the length of the first part of the undulator. Since it must be shorter than the saturation length of the fundamental harmonic in the first section, one can consider delaying the saturation of the fundamental with the help of phase shifters[8,9] in order to increase $L_{\mathrm{w}}^{(1)}$. However, for the sake of simplicity, we

did not use this option in our experiments.

Despite the bandwidth reduction factor (20) is significantly smaller than that of self-seeding schemes using optical elements[15–17], the HLSS FEL scheme is very simple and robust, and it does not require any additional installations, i.e. it can always be used in existing or planned gap-tunable undulators with a sufficiently large K-value.

One more advantage of the HLSS FEL scheme over the SASE FEL (and in many cases over a self-seeded FEL) is the possibility of a more efficient use of a post-saturation taper[40–42] for an improved conversion of the electron beam power to the FEL radiation power[14,45]. It is well-known[47] that a seeded (self-seeded) FEL works better in the post-saturation tapering regime than SASE FEL. In the latter case, a poor longitudinal coherence limits the length of the tapered part of the undulator to a length on which a slippage of the radiation with respect to the electron beam is comparable with the FEL coherence length[43,44]. In a self-seeded FEL the coherence length is much larger and it does not limit the performance of the tapered FEL (unless a sideband instability starts playing a role[40]). A disadvantage of a self-seeded FEL is that the saturation length is almost doubled with respect to the SASE regime, so that the available length for tapering the undulator may become too short. Considering now the HLSS FEL, we can state that it combines both advantages: coherence length is significantly larger than in the case of the SASE FEL, and the saturation length is shorter than that of the SASE FEL. In other words, there is more undulator length, available for tapering, than in the cases of the self-seeded FEL and SASE, and the longitudinal coherence is good enough to perform efficient tapering over this length. This makes us believe that HLSS FEL will become a standard mode of operation of X-ray FEL facilities.

Numerical simulations of the HLSS FEL were presented in[14] for the European XFEL[26] and in[45] for FLASH[27]. In this paper we report on the first operation of the harmonic lasing self-seeded FEL. The experiment was performed at the 2nd undulator line of the free electron laser FLASH[1,23,27]. We detected clear evidence of the 3rd harmonic lasing in the wavelength range from 4.5 nm to 15 nm and compared performance of HLSS FEL and SASE FEL. Obtained experimental results are in good agreement with expectations[14,45]: HLSS FEL provides more powerful photon beams with improved longitudinal coherence.

5. Operation of the HLSS FEL at FLASH2

The first soft X-ray FEL user facility FLASH[1,27] was upgraded to split the electron pulse trains between the two undulator lines so that the accelerator with maximum energy of 1.25 GeV now drives both lines. In a new separate tunnel, a second undulator line, called FLASH2, with a variable-gap undulator was installed, while a new experimental hall has space for up to six experimental stations[23]. The gap-tunable undulator of FLASH2 consists of twelve 2.5 m long sections with the undulator period of 3.14 cm and the maximum rms K-value about 1.9. This makes it possible

14

(see formula (2)) to study the HLSS FEL scheme with the 3rd harmonic seeding. Due to the parallel operation with FLASH1 undulator line, the invasive electron beam diagnostics, placed in the common part of the machine, was not available during the measurements. Moreover, FLASH2 is not equipped with the longitudinal beam diagnostics yet. For this reasons we can not directly compare our measurements with numerical simulations. We could, however, observe a good qualitative agreement with the simulations[45] that were done before the measurements. Below we present the experimental results published in Ref.[46].

5.1. *First lasing at 7 nm*

On May 1, 2016 we were able to successfully perform the first test of HLSS FEL at FLASH2. Electron energy was 948 MeV, charge 0.4 nC. Initially we tuned 10 undulator sections to a standard SASE, operating in the exponential gain regime at the wavelength of 7 nm (rms K parameter was 0.73); the pulse energy was 12 μJ. Then we detuned the first section, tuned it to the third subharmonic (rms K was 1.9) and scanned it around 21 nm. We repeated the measurements with the first two sections, and then with the first three sections. Note that the fundamental at 21 nm was also in the exponential gain regime, pulse energy after three undulator sections was 40 nJ, i.e. it was far away from saturation (which was achieved at the 200 μJ level). This means, in particular, that the nonlinear harmonic generation in the first part of the undulator is excluded.

One can see from Fig. 9 that the effect is essentially resonant. For example, in the case when three undulator sections were scanned, the ratio of pulse energies at the optimal tune, 21.1 nm, and at the tune of 20 nm is 51 μJ/0.3 μJ = 170. This ratio is likely underestimated because the background radiation at the fundamental at 20 nm (even being much weaker, about 40 nJ) is more efficiently detected by the microchannel plate (MCP) based detector[50,51] used in this measurement. Note that the MCP detector has a very large dynamical range and a high signal-to-noise ratio. For these reasons it is best suited to measurements of the FEL gain curve and statistical properties of the FEL radiation[1,49,57]. This detector has no absolute calibration, therefore in our experiments we used gas monitor detector (GMD)[52,53] to absolutely calibrate the MCP detector at the level of 10 μJ.

We claim that there can be only one explanation of the effect that we observe in Fig. 9: FEL gain at 7 nm is strongly reduced as soon as the first part of the undulator is detuned, and then the gain is recovered (and becomes even larger) due to the 3rd harmonic lasing in the first part as soon as the resonant wavelength is 21 nm.

We should stress that the pulse energy with three retuned undulator sections (51 μJ) is significantly larger than that in the homogeneous undulator tuned to 7 nm (it was 12 μJ). This is because the gain length of harmonic lasing is shorter than that of the fundamental tuned to the same wavelength (see formula (3), Fig. 2 and refs.[8,9,14,45]). A rough estimate gives us the ratio of gain lengths about 1.4 which
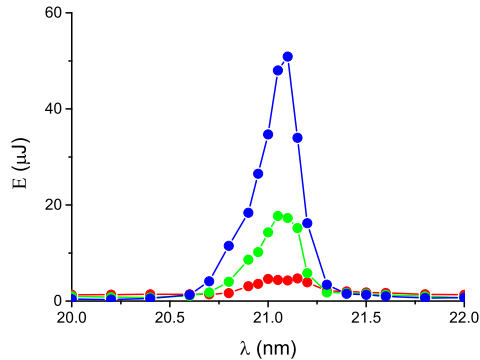
Fig. 9.   Scan of the resonance wavelength of the first part of the undulator consisting of one undulator section (red), two sections (green), and three sections (blue). Pulse energy is measured after the second part of the undulator tuned to 7 nm.

is somewhat smaller thah the ratio in Fig. 2. The difference can be explained by a contribution of the energy spread (not included in Fig. 2) and by the fact that the undulator beta-function was larger than an optimum value.

5.2. *Improvement of the longitudinal coherence at 11 nm*

We continued the studies of the HLSS FEL at FLASH2 in June 2016. Since the electron energy was different (757 MeV), we lased at another wavelength, 11 nm. We also used a different charge, 0.25 nC, in this experiment. The undulator settings were similar to the previous case: we used ten undulator modules, rms K-parameter was 0.73 in SASE mode and 1.9 in the first part of the undulator in HLSS mode. The difference with the previous measurements was that we detuned four undulator modules in HLSS regime.

In the same way as in the previous experiment, we performed the scan of the K parameter in the first part of the undulator and saw a resonance behavior again. In combination with the fact that the fundamental at 33 nm was by three orders of magnitude below saturation this proves that we had harmonic lasing at 11 nm in the first part of the undulator. The pulse energies were 11 μJ in SASE mode and 53 μJ in HLSS mode.

The main goal of this run was to demonstrate that HLSS scheme indeed helps to improve the longitudinal coherence of FEL pulses with respect to the standard SASE regime. One can do this by the demonstration of the bandwidth reduction and by the measurements of an increase of the coherence time.

The spectra were measured with the wide-spectral-range XUV spectrometer[54] of FLASH2. A narrow entrance slit is imaged by a 1200 l/mm spherical variable line spacing grating in the 5th grating order which allows for a resolution better than 0.01 nm. In Fig. 10 we present the averaged spectra for two study cases: SASE
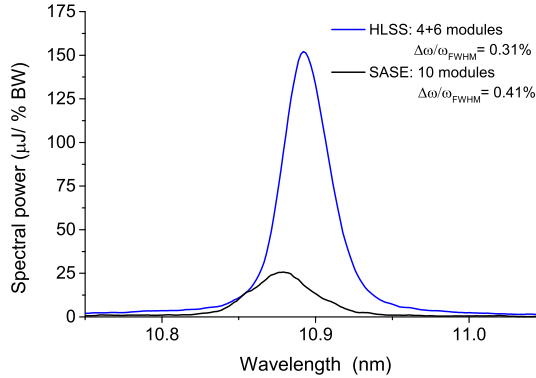
16

Fig. 10. Spectral density of the radiation energy for HLSS FEL configuration (blue) and for SASE FEL (black).

FEL with ten undulator modules and HLSS FEL with four modules tuned to 33 nm and six modules tuned to 11 nm. Let us note that a per cent level discrepancy between the measured wavelength (about 10.9 nm) and the wavelength expected by the undulator server (11 nm) comes from the fact that the server uses electron energy calculated from the RF vector sum and not from a direct measurement of the electron beam energy. However, the red shift of the radiation for the HLSS configuration with respect to the SASE case is real and can be explained by the fact that a seeded FEL radiates more efficiently in the case of a small red shift[35].

The spectra in Fig. 10 are the results of averaging over 50 single-shot spectra in each case. One can see that HLSS FEL indeed has a smaller bandwidth, 0.31%, as compared to 0.41% in the case of SASE FEL. The bandwidth reduction factor is 1.3 from this measurement. The spectral power, however, differs by a factor of six due to an additional increase of pulse energy in HLSS regime. This happens because the 3rd harmonic lasing at 11 nm has a shorter gain length than lasing at the same wavelength on the fundamental.

An expected bandwidth reduction factor (or coherence enhancement factor) R from formula (20) can be estimated at 1.7. The discrepancy can in a general case be explained by the energy jitter and/or energy chirp in the electron beam. The energy jitter effect is supposed to give a small contribution to the spectrum broadening since the FLASH accelerator was quite stable during the measurement, the energy stability can be estimated at the level of a few 10^{-4}. A contribution of the energy chirp, however, being converted to a frequency chirp within an FEL pulse, can be significant. The energy chirp appears in the accelerator on the one hand due to off-crest acceleration, needed for the bunch compression in magnetic chicanes, and on the other hand due to collective self-fields in the bunch (wakefields, longitudinal space charge)[1]. Both contributions can partially or fully compensate each other, this depends on accelerator settings. In the experiment we could tweak the
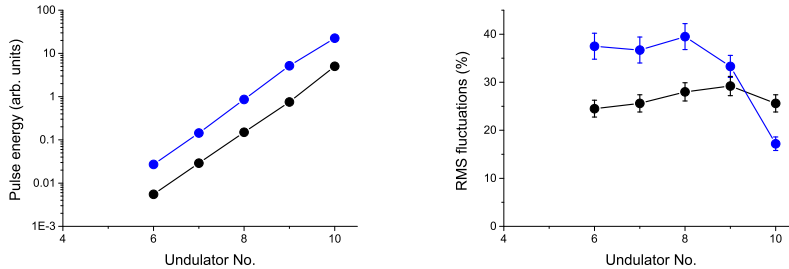
Fig. 11. Radiation pulse energy (left plot) and pulse energy fluctuations (right plot) in the second part of the undulator for HLSS (blue) and for SASE (black). Small aperture in front of the MCP detector is used in this measurement.

bunch compression, trying to minimize the HLSS FEL bandwidth, and we succeeded partially, the energy chirp was reduced to the 0.1% level.

Another method of determination of an improvement of the longitudinal coherence (independent of the presence of the frequency chirp in FEL pulses) is based on statistical measurements of the FEL pulse energy along the undulator length. It is well known[34,35] that in high-gain linear regime the radiation from a SASE FEL has a statistics of a completely chaotic polarized light[36]. Shot-to-shot rms fluctuations of the FEL pulse energy σ are connected with the number of modes by a simple relation: $M = 1/\sigma^2$. Number of modes can be represented as a product of the numbers of longitudinal, M_L, and transverse, M_T, modes. The latter is usually close to one, $M_T \simeq 1.1 - 1.2$ when a SASE FEL is well designed and optimized[55,56]. If one uses a small aperture to select only the central part of the FEL beam, the pulse energy fluctuations are a measure of the number of the longitudinal modes[49] : $M_L = 1/\sigma^2$. For a given FEL pulse length, the coherence length L_{coh} is inversely proportional to the number of the longitudinal modes, M_L. Making a reasonable assumption that the FEL pulse length is the same in both cases, HLSS and SASE, we end up with a simple ratio of coherence lengths for these two cases:

$$R = \frac{L_{coh}^{HLSS}}{L_{coh}^{SASE}} \simeq \frac{M_L^{SASE}}{M_L^{HLSS}} = \frac{\sigma_{HLSS}^2}{\sigma_{SASE}^2} \qquad (21)$$

In Fig. 11 we present the measurements of the FEL pulse energy and its fluctuations versus undulator length for a small aperture (significantly smaller than the FEL beam size) in front of the MCP detector. The measurements start behind the sixth undulator section because at this position the contribution of the background radiation at 33 nm is already negligible. In both cases, HLSS and SASE, the maximum of pulse energy fluctuations is achieved within the part of the undulator where the measurements were performed. However, in HLSS case the fluctuations drop down more significantly because the FEL enters nonlinear stage of amplification in this case. As one can see, in the linear regime of the FEL operation (sections 6 to

18

8) the fluctuations for HLSS case are visibly larger than in the SASE case. The validity of an assumption that pulse length in both cases is the same is justified by the fact that both FEL configurations were driven by the same electron beam under the same conditions. We did the measurements twice for each configuration to make sure that the results are not affected by any drifts in the accelerator. Thus, we can conclude that in the HLSS case we had a smaller number of modes, or a larger coherence length. Using formula (21) with the fluctuations measured behind the 8th undulator section for HLSS and the 9th section for SASE (at these positions with the largest fluctuations we have a similar gain in both modes), we obtain an estimate for the coherence enhancement factor in the end of the exponential gain regime: $R \simeq 1.8 \pm 0.3$. This is in a good agreement with already presented theoretical estimate $R \simeq 1.7$ obtained from (20).

Note that this moderate enhancement, observed in our experiment, is obtained because we are limited to application of the third (and not higher) harmonic at FLASH2. Further improvement can be done by increasing the length of the first part of the undulator (see formula (20)), making sure that the fundamental in the first part stays well below saturation (one can delay the saturation by using phase shifters as suggested in[8,9]). In a gap-tunable undulator with a higher K, like SASE3 undulator of the European XFEL (with the rms K about 7), one can, in principle, use a much higher harmonic number thus expecting a much higher coherence enhancement factor.

5.3. *A more efficient post-saturation taper at 15 nm*

In November 2016 we set up HLSS FEL as a configuration with four first undulators tuned to 45 nm and the last eight undulators tuned to 15 nm. The electron energy was 645 MeV, the charge was 100 pC, the rms value of K was 1.9 in the first part of the undulator and 0.73 in the second part. We reached FEL saturation in SASE and HLSS modes, and applied post-saturation taper to improve FEL efficiency[40–42].

Post-saturation taper in FLASH2 undulator is implemented as a step-taper (i.e. the undulator K changes from section to section but is constant within a section) with linear or quadratic law. We used quadratic taper and for each mode (HLSS and SASE) optimized two parameters: beginning of tapering and the taper depth. We ended up with the following optimized parameters: beginning of tapering was in the 9th (10th) undulator and the taper depth was 0.9% (0.7%) for HLSS (SASE). Pulse energy was enhanced for HLSS configuration from 18 μJ in non-tapered undulator to 31 μJ when post-saturation taper was applied. In case of SASE FEL the respective enhancement was from 15 μJ to 20 μJ. The pulse energy versus undulator length for both operation modes is presented in Fig. 12.

Note that a similar efficiency enhancement was previously observed in numerical simulations[14,45]. As it was discussed above, the improvement of post-saturation taper regime is achieved in HLSS case for two reasons: an earlier saturation and a better longitudinal coherence than in SASE case.
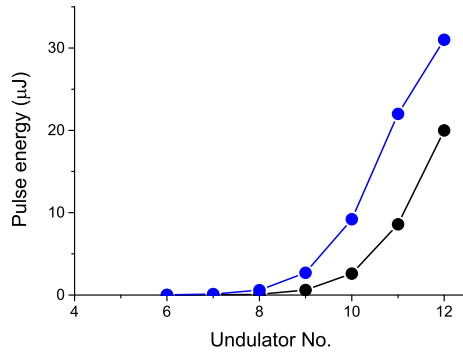
Fig. 12.   Radiation pulse energy versus position in the undulator for HLSS (blue) and for SASE (black). Post-saturation taper was optimized for both cases.
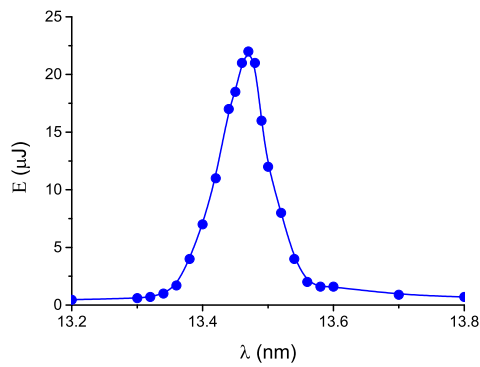

Fig. 13.   Scan of the resonance wavelength of the first part of the undulator consisting of three undulator sections. Pulse energy is measured after the second part of the undulator tuned to 4.5 nm and operated close to the FEL saturation.

5.4. *Lasing at 4.5 nm*

In September 2016 we were able to drive HLSS FEL by the electron beam with a higher energy, 1080 MeV, and thus obtain lasing at 4.5 nm in HLSS configuration. Initially, we tuned SASE regime with 12 active undulator sections (rms K value was 0.53), and could establish an onset of saturation with pulse energy at the level of 20 μJ. Then we tuned first three sections to 13.5 nm (increasing rms K value to 1.69), thus providing the third harmonic signal at 4.5 nm for seeding the last nine undulators. The scan of the undulator tune of the first three modules is presented in Fig. 13. The resonant behavior together with the fact that the fundamental at 13.5 nm was more than three orders of magnitude below saturation proves that we

20

had the third harmonic lasing at 4.5 nm in the first part of the undulator.

6. Conclusion

Harmonic lasing in a free electron laser with a planar undulator might be a cheap and efficient way of extension of wavelength ranges of existing and planned X-ray FEL facilities. Contrary to nonlinear harmonic generation, harmonic lasing can provide much more intense, stable, and narrow-band FEL beam which is easier to handle due to the suppressed fundamental. Another useful application of harmonic lasing is so called Harmonic Lasing Self-Seeded Free Electron Laser (HLSS FEL) that allows to improve spectral brightness of these facilities.

We were able to successfully demonstrate the harmonic lasing phenomena and the HLSS FEL principle at FLASH2 in the wavelength range between 4.5 and 15 nm. A change from SASE to HLSS configuration was very simple and fast, it worked well independently of a wavelength and accelerator settings. We can, therefore, forecast that HLSS may become a standard mode of operation of the X-ray FEL user facilities with gap-tunable undulators, providing an improvement of the longitudinal coherence, a reduction of the saturation length and a possibility of a more efficient post-saturation tapering.

It is also important to note that the first evidence of harmonic lasing in a high-gain FEL and at a short wavelength (down to 4.5 nm) paves the way for a variety of applications of this effect in X-ray FEL facilities[9,14,24,28].

References

1. W. Ackermann et al., Nature Photonics **1**(2007)336
2. P. Emma et al., Nature Photonics **4**(2010)641
3. T. Ishikawa et al., Nature Photonics 6 (2012) 540.
4. A.M. Kondratenko and E.L. Saldin, Part. Accelerators **10**(1980)207.
5. J.B. Murphy, C. Pellegrini and R. Bonifacio, Opt. Commun. **53**(1985)197
6. R. Bonifacio, L. De Salvo, and P. Pierini, Nucl. Instr. Meth. A293(1990)627.
7. Z. Huang and K. Kim, Phys. Rev. E, 62(2000)7295.
8. B.W.J. McNeil et al., Phy. Rev. Lett. 96, 084801 (2006)
9. E.A. Schneidmiller and M.V. Yurkov, Phys. Rev. ST-AB **15**(2012)080702
10. H. Freund, S. Biedron and S. Milton, Nucl. Instr. Meth. A 445(2000)53.
11. E.L. Saldin, E.A. Schneidmiller and M.V. Yurkov, Phys. Rev. ST-AB 9(2006)030702
12. A. Tremaine et al., Phy. Rev. Lett. 88, 204801 (2002)
13. D. Ratner et al., Phys. Rev. ST-AB 14(2011)060701
14. E.A. Schneidmiller and M.V. Yurkov, "Harmonic Lasing Self-Seeded FEL", Proc. of FEL2013, New York, p.700
15. J. Feldhaus et al., Optics. Comm. 140, 341 (1997).
16. E.L. Saldin, Y.V. Shvyd'ko, E.A. Schneidmiller and M.V. Yurkov, Nucl. Instrum. and Methods **A 475**(2001)357
17. G. Geloni, V. Kocharyan and E.L. Saldin, Journal of Modern Optics **58**(2011)1391
18. W.B. Colson, IEEE J. Quantum Electron. 17(1981)1417
19. S.V. Benson and J.M.J. Madey, Phys. Rev. A39(1989)1579
20. R.W. Warren et al., Nucl. Instr. Meth. A 296(1990)84

21. R. Hajima et al., Nucl. Instr. Meth. A 475(2001)43
22. N. Sei, H. Ogawa and K. Yamada, Journal of the Physical Society of Japan 79(2010)093501
23. B. Faatz et al., New Journal of Physics, 18(2016)062002
24. R. Brinkmann, E.A. Schneidmiller, J. Sekutowicz and M.V. Yurkov, Nucl. Instrum. and Methods **A 768**(2014)20
25. G. Penn, Phys. Rev. ST Accel. Beams 18, 060703 (2015)
26. M. Altarelli et al. (Eds.), XFEL: The European X-Ray Free-Electron Laser. Technical Design Report, Preprint DESY 2006-097, DESY, Hamburg, 2006 (see also http://xfel.desy.de).
27. S. Schreiber and B. Faatz, "The free-electron laser FLASH", High Power Laser Science and Engineering, 3, e20 doi:10.1017/hpl.2015.16
28. E.A. Schneidmiller and M.V. Yurkov, Nucl. Instrum. and Methods **A 717**(2013)37
29. E.L. Saldin, E.A. Schneidmiller and M.V. Yurkov, Opt. Commun. **235**(2004)415
30. E.L. Saldin, E.A. Schneidmiller and M.V. Yurkov, New Journal of Physics **12**(2010)035010
31. M. Xie, "Design optimization for an X-ray free electron laser driven by SLAC linac", Proceedings of the Particle Accelerator Conference 1995, Dallas, [http://www.jacow.org]
32. M. Xie, Nucl. Instrum. and Methods **A 445**(2000)59
33. R. Bonifacio, C. Pellegrini and L.M. Narducci, Opt. Commun. **50**(1984)373
34. E.L. Saldin, E.A. Schneidmiller and M.V. Yurkov, Opt. Commun. **148**(1998)383
35. E.L. Saldin, E.A. Schneidmiller and M.V. Yurkov, "The Physics of Free Electron Lasers", Springer, Berlin, 1999
36. J. Goodman, Statistical Optics, (John Wiley and Sons, New York, 1985).
37. J. Wu, J., A. Marinelli and C. Pellegrini, Proceedings of the 32th International Free Electron Laser Conference, Nara, Japan, 2012, p. 23, [http://www.jacow.org]
38. B.W.J. McNeil, N.R. Thompson and D.J. Dunning, Phys. Rev. Lett. 110(2013)134802.
39. D. Xiang et al., Phys. Rev. ST-AB **16**(2013)010703
40. N.M. Kroll, P.L. Morton, and M.N. Rosenbluth, IEEE J. Quantum Electron. 17, 1436 (1981).
41. W.M. Fawley, Nucl. Instrum. Methods Phys. Res., Sect. A 375, 550 (1996).
42. E.A. Schneidmiller and M.V. Yurkov, Phys. Rev. ST-AB **18**(2015)030705
43. E.A. Schneidmiller and M.V. Yurkov, The universal method for optimization of undulator tapering in FEL amplifiers, Proc. SPIE 9512, Advances in X-ray Free-Electron Lasers Instrumentation III, 951219 (May 12, 2015); doi:10.1117/12.2181230.
44. E.A. Schneidmiller and M.V. Yurkov, Optimization of a High Efficiency Free Electron Laser Amplifier, Proc. FEL2015 Conference, Daejeon, Korea, 2015, MOC02.
45. E.A. Schneidmiller and M.V. Yurkov, Proceedings of IPAC2016, Busan, Korea, p. 725, [http://www.jacow.org]
46. E.A. Schneidmiller et al., Phys. Rev.AB **20**(2017)020705
47. W.M. Fawley, Z. Huang, K.-J. Kim, and N.A. Vinokurov, Nucl. Instrum. Methods Phys. Res., Sect. A 483, 537 (2002).
48. E.A. Schneidmiller and M.V. Yurkov, Proceedings of IPAC2016, Busan, Korea, p. 722, [http://www.jacow.org]
49. E.A. Schneidmiller and M.V. Yurkov, Proceedings of IPAC2016, Busan, Korea, p. 738, [http://www.jacow.org]
50. A. Bytchkov et al., Nucl. Instrum. and Methods A 528 (2004)254.
51. O. Brovko et al., Proc. IPAC2016, Busan, Korea, 2016, mopow014.
52. K. Tiedtke et al., J. Appl. Phys. 103, 094511 (2008)

22

53. K. Tiedtke et al., New J. Phys. 11 (2009) 023029
54. T. Tanikawa et al., Nucl. Instrum. and Meth. A 830, 170-175 (2016)
55. E.L. Saldin, E.A. Schneidmiller, and M.V. Yurkov, Opt. Commun. 281(2008)1179.
56. E.L. Saldin, E.A. Schneidmiller, and M.V. Yurkov, New J. Phys. 12 (2010) 035010
57. C. Behrens et al., Phys. Rev. ST Accel. Beams 15 (2012) 030707.